

**Bombay Plume transport, structure and microphysical interactions over the
Arabian Sea during Indian Winter Monsoon.**

Andrew Martin

Florida State University

NASA-GSFC/UMBC-JCET GSSP

Summer 2007

Abstract:

The Nature of the Bombay Plume during the winter monsoon months of December-January-February (DJF) was examined for the period 2003-2007. Particular attention was paid to the spatial extent and temporal persistence of the phenomenon, the plume's vertical structure, and effects by plume aerosols on sea surface temperatures and hydrometeors over the nearby eastern Arabian Sea. The plume was determined to contain high concentration of anthropogenic aerosols, with a persistent source region located in the Western Indian province of Maharashtra near the cities of Mumbai and Pune. During northeasterly flow regimes typical of Indian Winter Monsoon, high aerosol optical depths extend well into the Arabian Sea. Strong plume events over the Arabian Sea typically persist for around 5 days, with a frequency on the synoptic timescale. The plume was found to be very shallow during northeasterly flow regimes, with aerosols sinking as they are transported over the ocean. A strong correlation was found between high aerosol depths and low anomaly sea surface temperatures in the Arabian Sea during plume events. In addition, effective cloud drop radii distribution was observed to narrow in the presence of high aerosol concentration. Mean cloud optical depths were observed to increase in the presence of high aerosol concentration.

Introduction:

Interest in aerosol transport over South and Southeast Asia has increased as the area has experienced a growth in heavy industry. The Western Indian cities of Mumbai and Pune are examples of this growth, and contain a high concentration of technology/general industry manufacturers (Gradel, Kutzen, 1993). These cities are a source of anthropogenic aerosols such as CO and VOC's (Black carbons) as well as NO_x and O₃ (Phadnis, Levy, Moxim, 2002). In previous studies, transport of black carbon rich air from Western/Northwestern India over the Arabian Sea has been described as the "Bombay Plume" (Lobert & Harris, 2002; Lelieveld et. al. 2001). While the phenomenon has been identified, the atmospheric conditions which lead to Bombay Plume (BP), its vertical structure, and its effects on physical parameters over the ocean are unclear. This study will identify cases of aerosol loading over the Eastern Arabian Sea (EAS) near the

cities of Mumbai/Pune, India using the Moderate Resolution Imaging Spectroradiometer (MODIS) instruments aboard NASA's terra/aqua satellites. This study will identify the atmospheric conditions/flow regimes that contribute to the BP using NCEP reanalysis wind data. The study will examine vertical structure/extent of the BP using the 1064 nm LIDAR backscatter detector on board NASA's Cloud-Aerosol Lidar and Infrared Pathfinder Satellite Observation (CALIPSO) satellite. The study will also show the effect aerosols from the BP have on sea surface temperature, and cloud hydrometeor properties over the EAS via parameter composites of BP cases from 2003-2007 and Probability Distribution Functions (PDF's) derived from MODIS and observations from NASA's Tropical Rainfall Measurement Mission (TRMM). This paper will present these results and discuss the nature of the Bombay Plume and its effect on atmospheric conditions over the nearby ocean as the first step in a verification of analyses from the GEOS-5 regional model and GOCART aerosol transport model developed by NASA-Goddard Space Flight Center (GSFC).

Observations:

Observations for this study were provided by MODIS, CALIPSO and TRMM satellite remote sensing instruments, as well as NCEP's global reanalysis products. MODIS provided primary data for resolving the BP and tracking it across the EAS. MODIS consists of a 36 channel spectroradiometer. Nine channels of approx. 20nm bandwidth in the infrared spectral region are used to resolve aerosol properties. An additional 8 channels covering more bandwidth in the higher wavelengths (near infrared and visible) are used to resolve cloud properties. The MODIS spectroradiometer is carried on two Earth Observing System (EOS) satellites: terra and aqua. Terra makes descending polar-orbiting passes over the tropic of cancer near 10:30 local time. Likewise Aqua passes in ascending orbit near 13:30 local time. (Maccherone). The MODIS atmosphere group uses algorithms to create a combined land-ocean mean total aod (optical depth at 0.55 micron), aerosol mean particle size, and fine particulate (radius < 0.5 μm) to coarse particulate (radius > 1.0 μm) ratio (Hubanks, 2007). In addition, MODIS observed spectral radiance and cloud mask grids can be used to calculate several cloud optical properties for grid squares in which clouds are present. Through lookup

table algorithms, MODIS makes available cloud optical thickness and effective cloud drop radius. MODIS is designed to have spatial resolution of 0.5 km for the aerosol resolving channels, and 1 km for cloud product channels. (Hubanks, 2007); however, this high resolution is regridded to 1 degree latitude resolution and made available in an HDF archive.

MODIS can resolve aod over oceans and dark vegetated land surfaces, but does not provide data over deserts or ice. In addition, the length resolved transverse to the orbital path (footprint) from consecutive passes do not overlap (Lorentz, 2007). Thus, the daily data from each satellite contains gaps which make resolving the entire BP on any given day difficult. Because the BP is a local feature on a small spatial and temporal scale, (only over the EAS for 3-7 days) we combined the aod grids from both terra and aqua to create our principal dataset. A simple point by point arithmetic mean of aod was taken, excluding the points for which terra and aqua data did not overlap.

Data from CALIPSO provided information about the vertical extent and structure of the BP. CALIPSO carries a LIDAR instrument (CALIOP) which measures backscatter from aerosols and cloud droplets in the visible light range. The satellite follows the same orbit as the MODIS Aqua satellite, lagging by about 2 minutes (Lorentz, 2007). The LIDAR instrument on CALIPSO is capable of measuring aerosol vertical profiles, and aerosol optical depth. Unlike MODIS, CALIPSO's footprint is virtually zero-width. Therefore CALIPSO is useful for determining vertical profile information, but cannot provide information about horizontal distribution of aerosol parameters.

Vertical extent and distribution of relative backscatter radiances in an aerosol feature can be retrieved directly from the CALIPSO website in the form of vertical cross-section images.

In addition to MODIS cloud and aerosol products, TRMM data was needed to study the interaction between aerosols of the BP and hydrometeors and sea surface temperature (sst) over the EAS. TRMM contains many instrument packages focused on measuring tropical rainfall. The TRMM Microwave Imager (TMI) provided sst and cloud liquid water (clw) grids. TMI is a passive microwave sensor. Over the ocean, TMI resolves atmospheric water by its emission curve with the help of the cold background dimming property of large bodies of water (Adler, 2006). Large bodies of water appear

dimmer in the microwave region than Planck's law predicts, but microwave emission from water (liquid and vapor) suspended in the atmosphere largely follows its predicted Planck curve (Adler, 2006). Thus, TMI only takes measurement over the oceans. The TRMM satellite has an eccentric orbit which only takes it between 35 N and 35 S latitude. As with terra/aqua, it takes several passes for complete global coverage from TRMM.

Data Manipulation:

Sea Surface Temperature follows an annual cycle of cooling and warming driven not only by solar radiation and sensible heat, but also by seasonal upwelling caused by flow at the air/sea boundary. Possible fluctuations in sst caused by aerosol solar dimming are likely to be fairly small in comparison. The Arabian Sea shows complicated patterns of upwelling which make discerning a change in sst during a short lived event such as the Bombay Plume difficult.

The annual cycle fluctuation of sea surface temperature in the area was removed by creating a time-series of sea-surface temperatures at each grid point over 9-years 1999-2007 of TMI data. A fourier transform of the time-series was performed, and the first four moments of the fourier-transform were removed. The "zeroth" moment corresponds to the 9-year mean sst. The first moment was assumed to correspond to the annual solar cycle, and the second to the annual upwelling cycle. The third moment would then correspond to upwelling caused by flow cycles on a seasonal timescale. The resulting data was assumed to be the anomaly departure in sst caused by changes on a weekly scale. This corresponds to the average duration of a typical BP event. (see Plume Transport section) The anomaly data was used in creating sst composites, and in creating probability distributions of sst.

Plume Transport:

This study was particularly interested in aerosol interactions over the ocean, as data coverage from both MODIS and TRMM is better over ocean. Mumbai sits on the Middle Western coast of India on the Eastern Arabian Sea. Studies by Krishnamurti have identified the dominant flow in the region at lower levels as northeasterly during winter

monsoon months (Krishnamurti et al, 1997). This should tend to push aerosols created in Mumbai and Pune out to sea and to the southwest. As this flow is well-documented, the task of this study was not to prove that aerosols move southwest over the Arabian Sea, but to identify Mumbai/Pune as the source region of these particles. To this end, a case list was compiled of “typical” Bombay Plume events during D-J-F from 2003-2007. This period was chosen because aod data was available from both terra and aqua satellites. A typical event needed to satisfy two criteria. First, the aerosol depth exceeded .35 from an areal average between 67 to 72 E longitude and 13 to 18 N latitude. In addition, to be a typical event, winds from NCEP reanalysis had to be northeasterly for 3 or more days surrounding peak aod. From this case list, two attributes of the Bombay Plume were immediately apparent. A typical winter monsoon plume event lasts around 5 days. This can be seen in a time-series (Fig. 1). Also, the low-level flow that drives a typical event is caused by an Arabian surface high pressure system, in conjunction with low pressure at the surface near the Maldives. These features are seen in the composite of winds and 925 mb heights from the case list. (fig. 2)

A composite of average aod and 925 mb winds was made from the case list by averaging the parameters over all cases during the central event day, one day prior, two days prior, 1 day after, and two days after the event. This was done for total aod (fig 3a) and fine mode aod (fig 3b). The day-by-day perturbation composite of total aod is shown in figure 4. Values in the perturbation correspond to the previous total aod composite with the 5-day mean subtracted.

The composites show that the BP originates in West Central India near Mumbai and Pune two days prior to the highest aod concentrations over the EAS. A typical Bombay Plume may take a northward turn towards the Gulf of Cambay before being caught in a low level jet (see fig 2) which speeds transport to the southwest. The fine mode composites show that the BP contains a proportionally high concentration of small (< 0.5 micron) particles. Particles of this size are likely of anthropogenic origin (Hubanks, 2007). This is in contrast to high aod regions near the Arabian Peninsula which diminish in the fine mode composites.

The composites show the BP following the low-level wind flow in general. The peak perturbation aod is transported farther out to sea over a period of 5 days, and dissipates soon after.

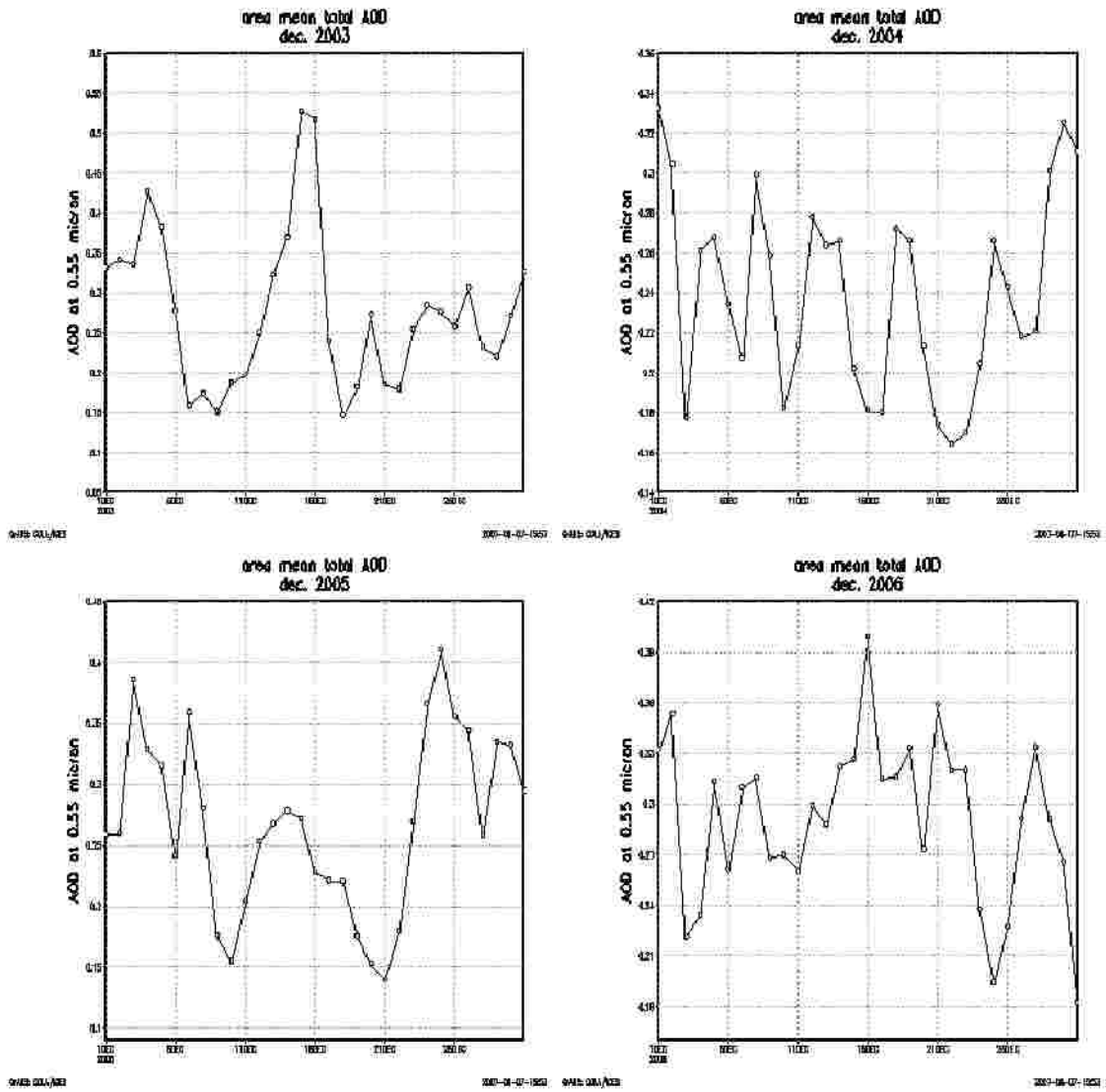


Figure 1: Time Series of area mean total AOD (at 550 nm) for 67-72 E, 13-18 N for December 2003-2006.

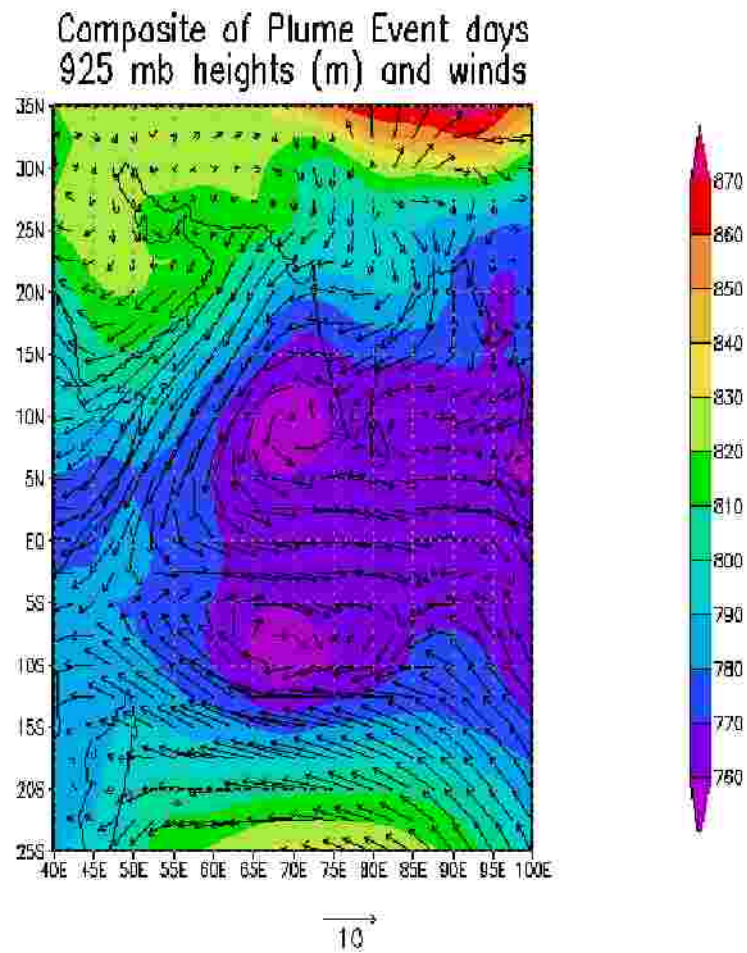
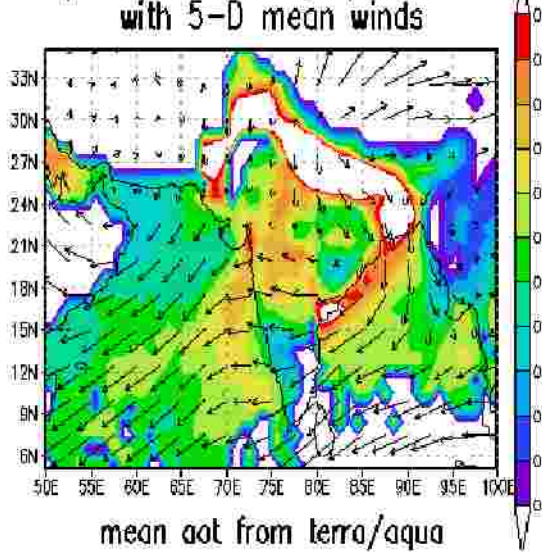
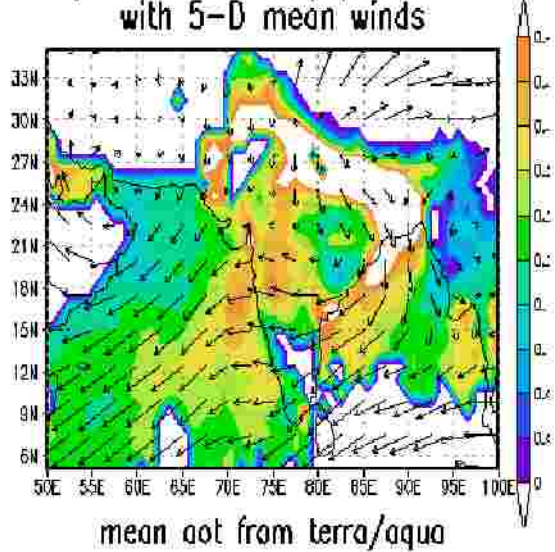


Figure 2: Composite 925 mb winds and geopotential heights for all Bombay plume events 2003-2007 during D-J-F.

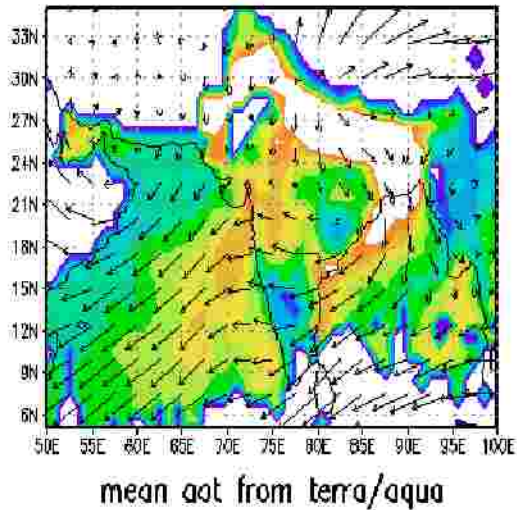
Composite AOD 2-days prior to event
with 5-D mean winds



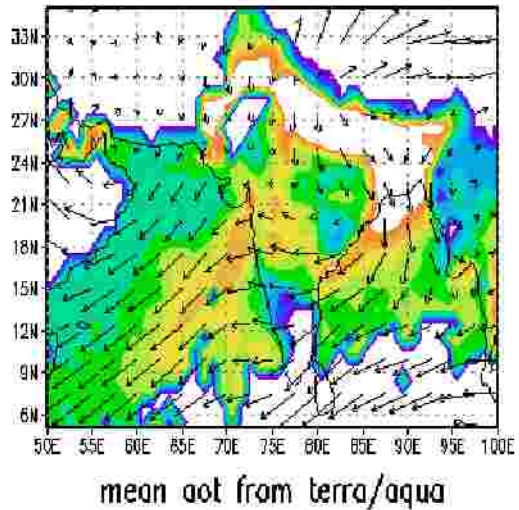
Composite AOD 1-day prior to event
with 5-D mean winds



Composite AOD event days
with 5-D mean winds



Composite AOD 1-day after event
with 5-D mean winds



Composite AOD 2-days after event
with 5-D mean winds

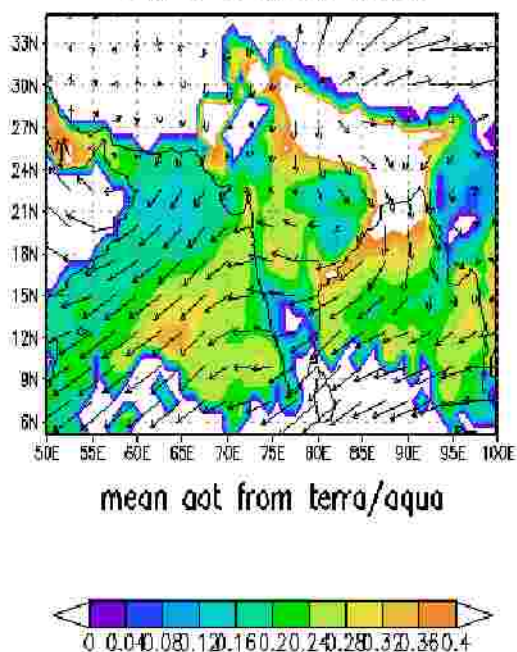
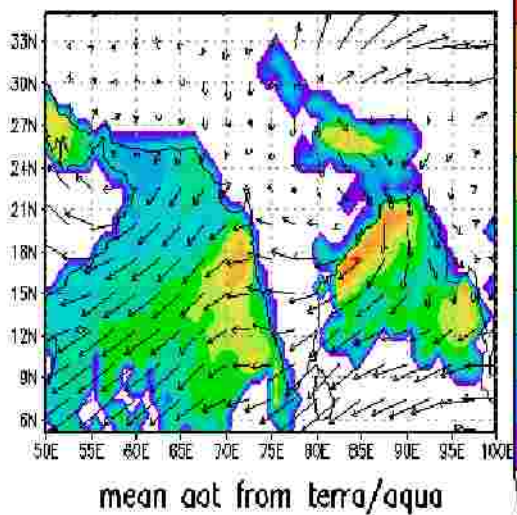
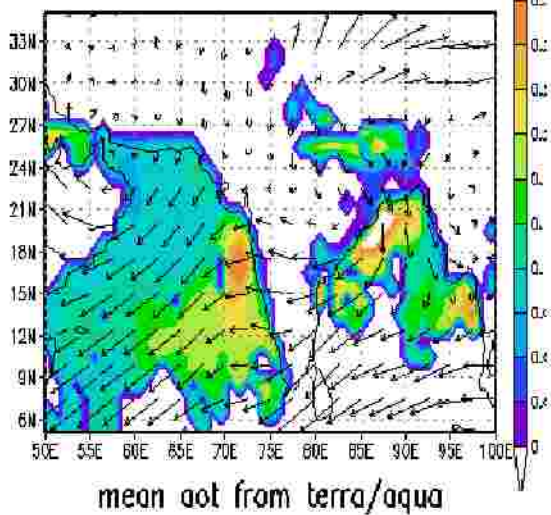


Figure 3a: Composites of total AOD (at 550 nm) and 5 day mean 925 mb winds for each day of plume cases 2003-2007 during D-J-F.

Composite AOD 2-days prior to event
with 5-D mean winds



Composite AOD 1-day prior to event
with 5-D mean winds



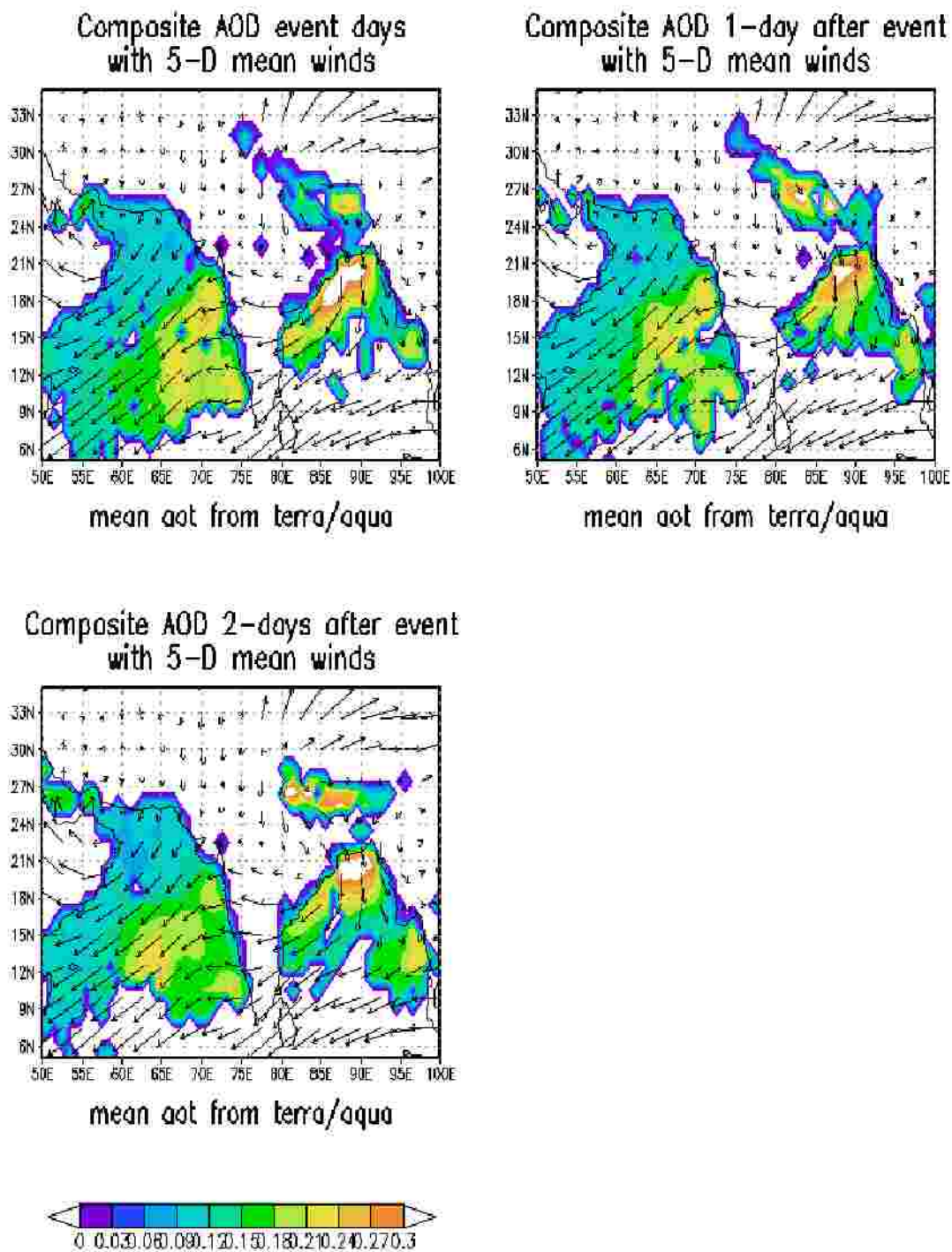
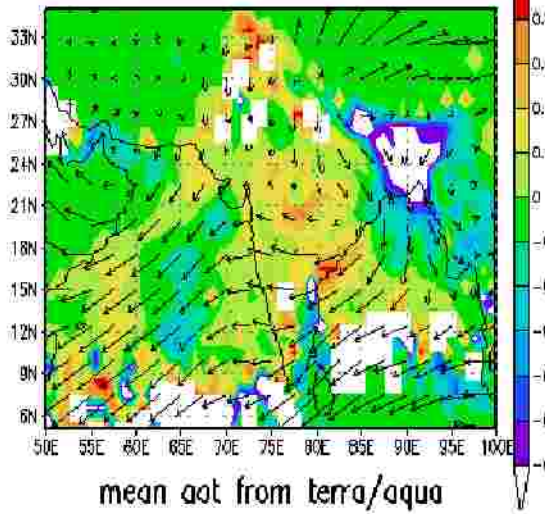
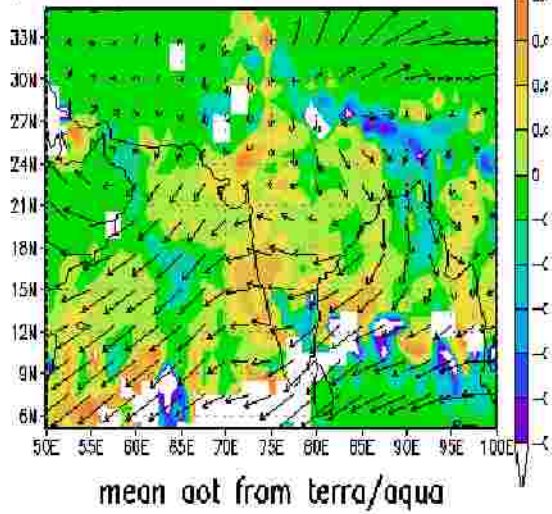


Figure 3b: Composites of fine AOD and 5 day mean 925 mb winds for each day during plume cases 2003-2007 during D-J-F.

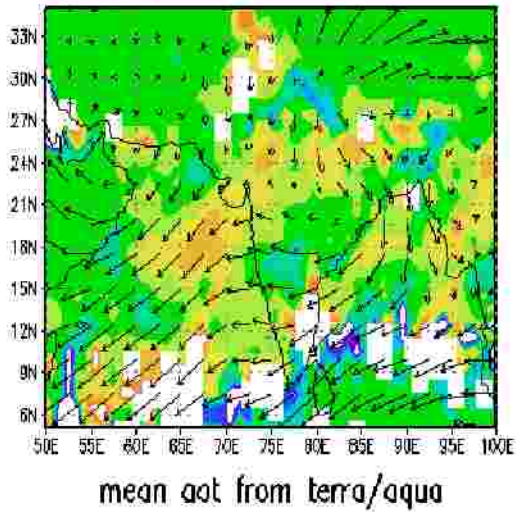
Composite perturbation AOD 2-days prior to event with 5-D mean winds



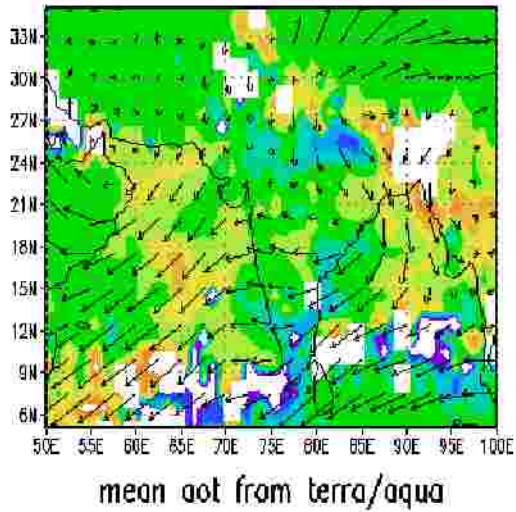
Composite perturbation AOD 1-day prior to event with 5-D mean winds



Composite perturbation AOD event days with 5-D mean winds



Composite perturbation AOD 1-day after event with 5-D mean winds



Composite perturbation AOD 2-days
after event with 5-D mean winds

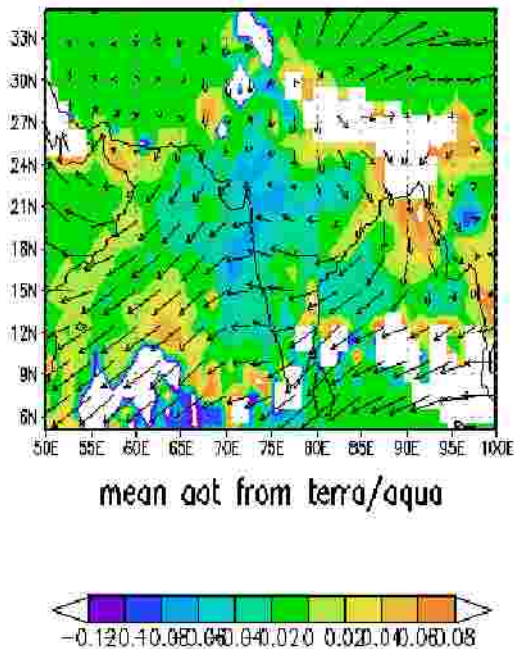


Figure 4: Composites of perturbation AOD and 5 day mean 925 mb winds for each day during plume cases 2003-2007 during D-J-F.

Vertical Extent:

CALIPSO has been in operation only since mid-June of 2006. Only three cases of “typical” D-J-F Bombay Plumes occurred in the intervening period. CALIPSO was overhead on a relatively clear day for two of these. Good images of the BP exist for December 5, 2006, and for January 9 and 11, 2007. Clear conditions in the mid and upper levels are important for resolving the BP with the CALIPSO instrument as the instrument relies on visible light backscattering, and can only penetrate very thin clouds. Due to the small vertical extent of the BP, the lidar must nearly reach the surface to resolve the plume. Figures 5 a-c show that The Bombay Plume exists only below 3 km, and is even lower for the CALIPSO passes further over the ocean. This is consistent with the conditions over Western India during D-J-F. During this period, convective stability is high, and subsidence is present as the prevailing flow moves from land to ocean. (Krishnamurti et. Al, 1997). Because of the subsidence, and the length of path over the

Arabian Sea, it is likely that most aerosols in the plume are deposited in the ocean during the winter months.

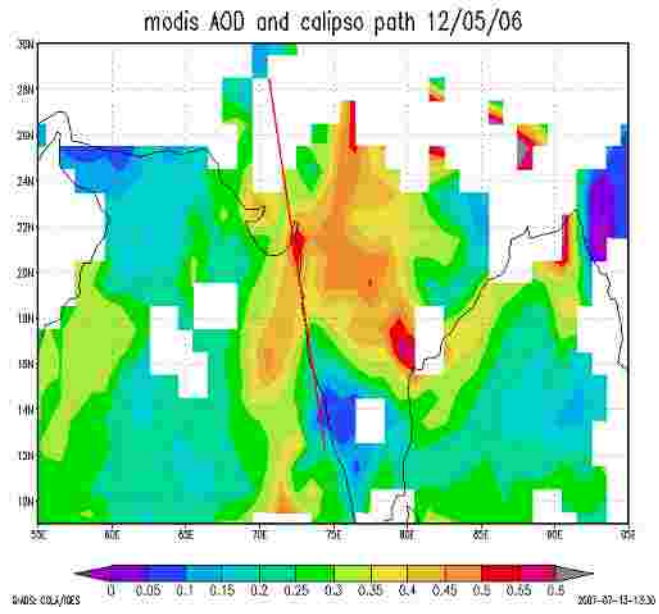
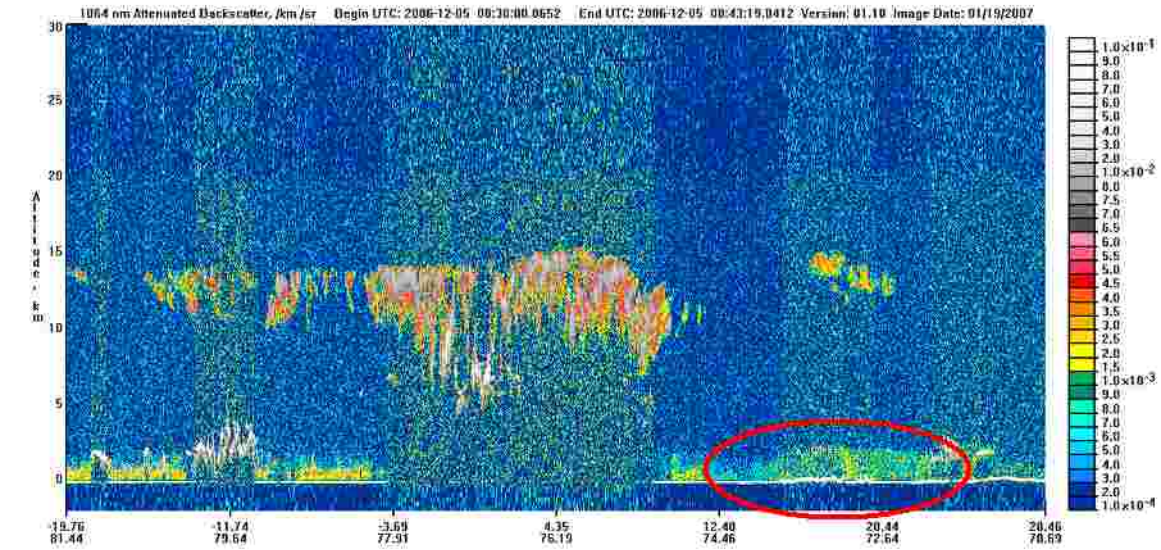


Figure 5a: Top: Vertical backscatter from calipso from Dec 5 2006 (plume circled in red). Bottom: Plan view of Calipso's path (red line) over AOD on Jan 9 2007.

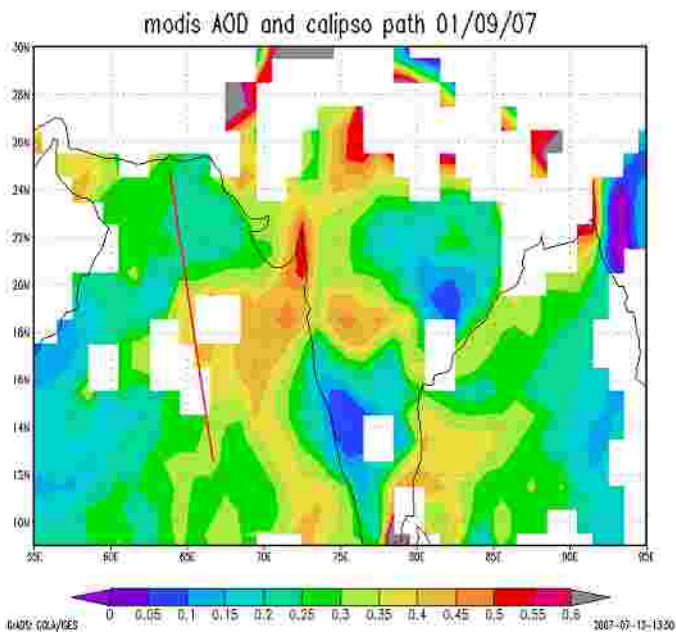
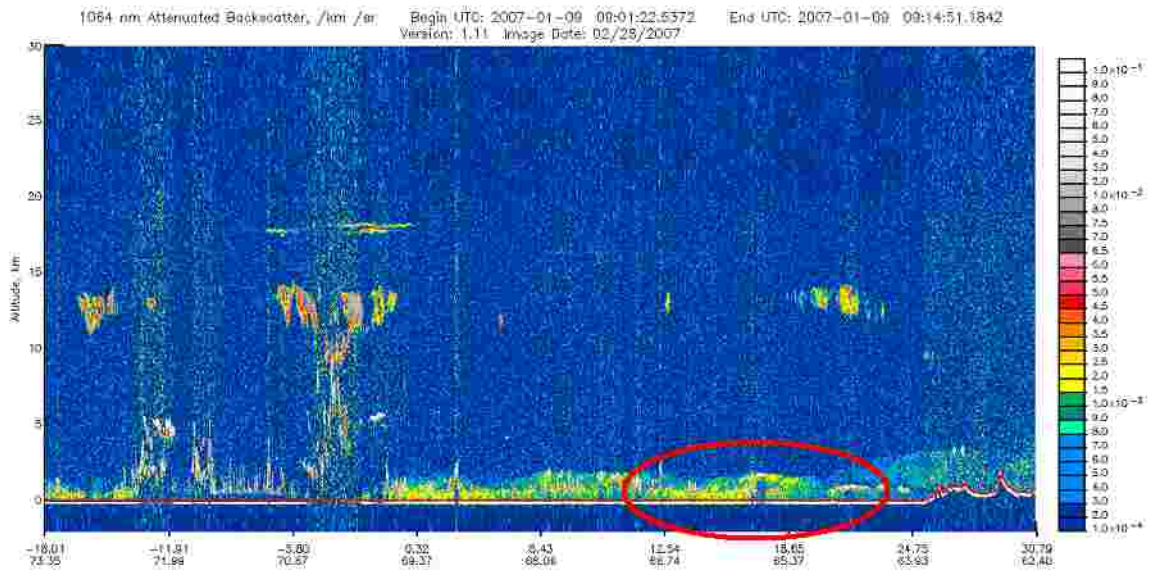


Figure 5b: Top: Vertical backscatter from calypso from Jan 9 2007 (plume circled in red). Bottom: Plan view of Calipso's path (red line) over AOD on Jan 9 2007.

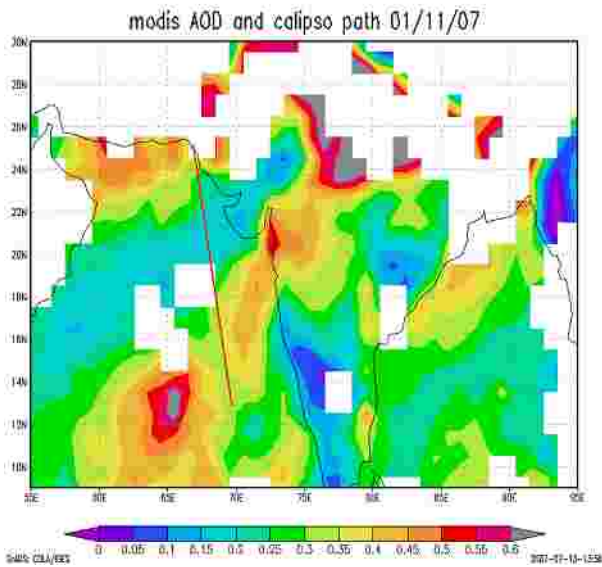
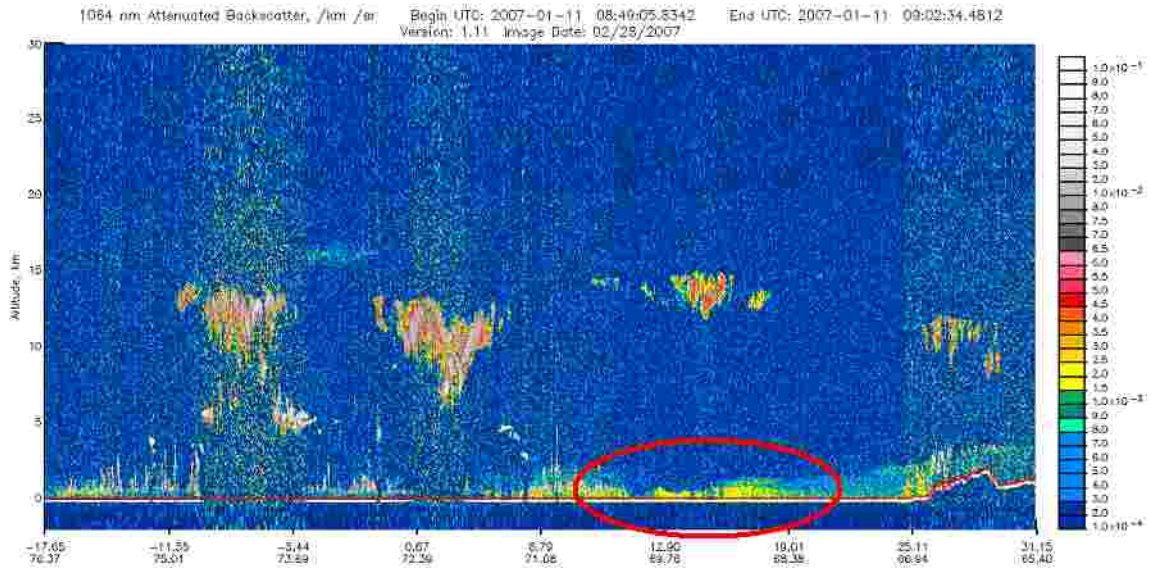


Figure 5c: Top: Vertical backscatter from calipso from Jan 11 2007 (plume circled in red). Bottom: Plan view of Calipso's path (red line) over AOD on Jan 11 2007.

Interactions With the Arabian Sea Environment:

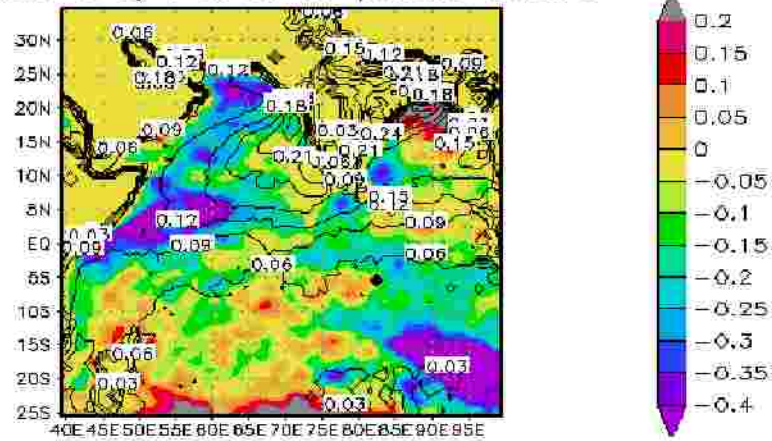
During prevailing winter monsoon flow regimes, it is likely that the aerosols from the Bombay Plume have the highest impact on the Arabian Sea. Aerosol particles suspended in the atmosphere have the effect of reducing the amount of solar radiation reaching the surface. Many aerosol species such as black carbon and sulfates are strong absorbers of visible and near visible wavelengths. Other species including dust and sea salt scatter incoming solar radiation. This has the effect of reducing the light that can

penetrate below the scattering particles. (Lau & Kim, 2007; Rathmanathan, 2005) This altering of the atmospheric radiation budget by aerosols has been studied extensively. It has been linked to an “Elevated Heat Pump” over the Tibetan Plateau, and the weakening of tropical cyclones caused by lower sea surface temperatures (Lau & Kim, 2006; 2007).

It appears that the Bombay Plume also serves to lower ssts in the EAS. Figure 6 shows two composites of anomaly sst averaged over all typical cases. The 5-day average of anomaly sst during plume events is compared to the average sst during the 5-days before the plume event. The cooling during the passage of the plume is dramatic. Some areas directly beneath the plume experience a drop of greater than one-tenth degree Celsius. This result is reinforced by a probability distribution for anomaly ssts in the plume area over fifteen days surrounding plume events (fig. 7). Values from each grid point in the plume area are placed in linear bins according to their anomaly sst. The fifteen days are broken into 3 time periods: 5 days before a plume event, 5 days during the plume event, and 5 days after the plume event has passed. The distribution drifts toward cooler temperatures in chronological order. After the first 5 days, when the plume is firmly established over the EAS, the mode value has cooled 0.2 deg Celsius. The mode of the probability distribution continues to cool for the next 5 days by an additional 0.1 degree Celsius. In contrast, a probability distribution for aod in the plume area (fig. 8) shows the aod increasing during plume events, but returning to its previous value in the next 5-day period. The aod distributions were created using decaying exponential bin spacing. This is consistent with the extinction of solar radiance (and thus surface heating) as light passes through scattering/absorbing particles. $\Delta R \propto 1 - \exp(-AOD)$. (Kaufman et al, 2005)

While these results are dramatic for a slow-response parameter such as sea surface temperature, this paper does not propose that the cooling observed during Bombay plume passage is due to radiative dimming alone. There is a moderate low level jet associated with the Bombay Plume which is also capable of significant sst cooling.

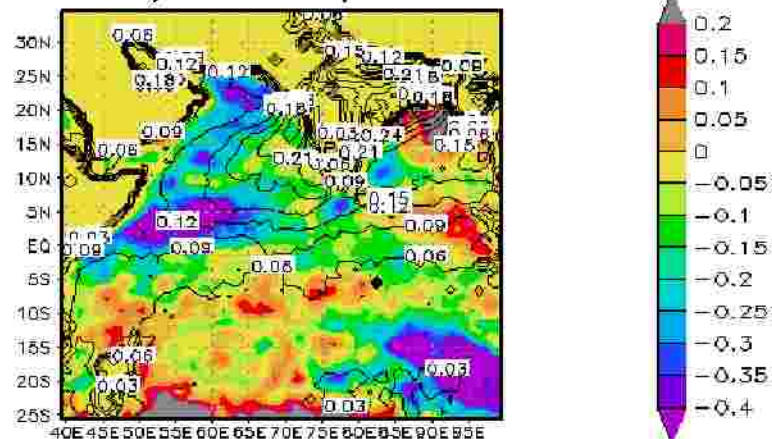
composite of 5-d mean anomaly ssts
(with aod) PRIOR to plume events



GrADS: COLA/IGES

2007-07-23-14:58

composite of 5-d mean anomaly ssts
(with aod) DURING plume events



GrADS: COLA/IGES

2007-07-23-14:58

Figure 6: Top: Composite of SST (shaded) for 5 days prior to plume passage (over all plume events 2003-2007 during D-J-F) with total AOD in black contours.
Bottom: Composite of SST (shaded) for 5 days surrounding plume passage (over all plume events 2003-2007 during D-J-F) with total AOD in black contours.

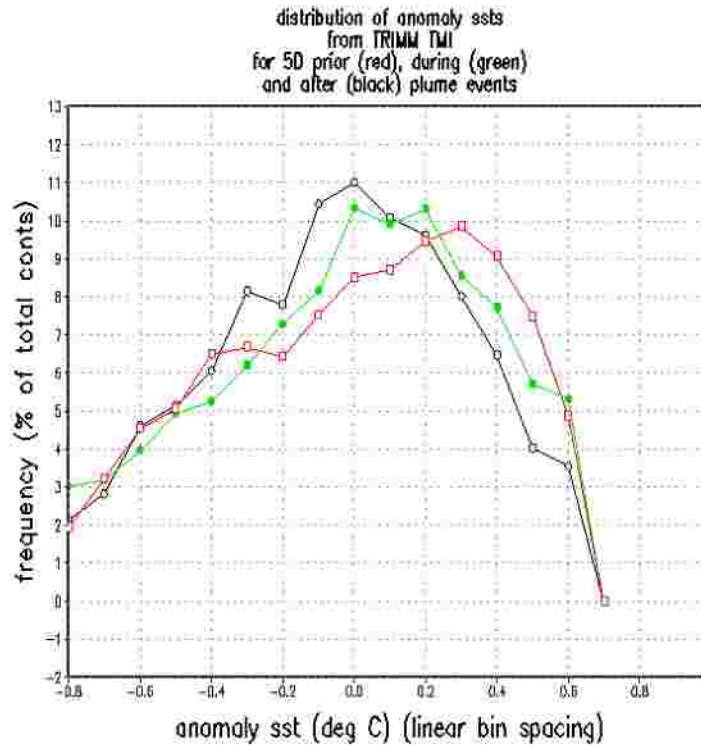


Figure 7: probability distribution of ssts in plume area for all plume events 2003-2007 during D-J-F. Red curve: 5 days prior to plume passage. Green curve: 5 day period surrounding plume events. Black curve: 5 day period after plume passage.

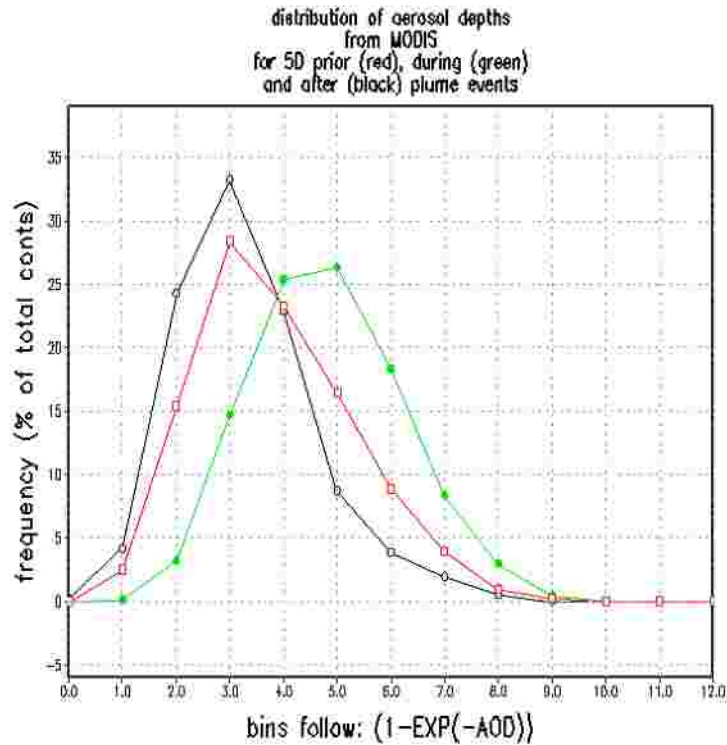


Figure 8: probability distribution of aod in plume area for all plume events 2003-2007 during D-J-F. Red curve: 5 days prior to plume passage. Green curve: 5 day period surrounding plume events. Black curve: 5 day period after plume passage.

Hydrometeor Interaction:

It is accepted that atmospheric aerosols can have a large impact on cloud formation and microphysics. These aerosol indirect effects in turn impact rainfall, cloud persistence, and the portion of earth's radiation budget which is affected by clouds. (Takemura et al, 2007) Certain aerosol species serve as cloud condensation nuclei (CCN), and are thought to narrow the droplet size distribution within a cloud. In the presence of high CCN concentration, formation of cloud droplets becomes possible at lower supersaturations. However, since fewer drop sizes are available within the cloud, collision/coalescence processes may not be as efficient in growing very large drops. This is known as the aerosol second indirect effect. The second indirect effect may lead to suppression of precipitation, and persistence of low clouds. (Kaufman et. al. 2005) Cloud persistence often leads to a positive correlation between aerosol and cloud thickness when measured on a large scale, and averaged over time. (fig. 9)

Probability distributions for cloud effective radius (cer) and cloud optical depth (cod) were created in a different fashion from those involving aod and sst. Since the BP was observed to exist only at low levels, only parameters of liquid phase clouds were extracted from the MODIS data. Also, it was observed that over our study area MODIS cloud will sometimes assign cer and cod values to grid points that contain clear sky according to TRMM or ground-based observations. This behavior may be related to sunglint problems over tropical oceans (Platnick, 2003). In order to guard against including clear sky grid points in the distribution, TRMM cloud liquid water data was used as a cloud mask. If the grid square to be counted had a cloud liquid water content of greater than 0.04 g/kg according to TRMM, the point was considered valid for inclusion in the distribution. If not, the grid point was discarded.

A treatment involving comparisons over successive 5-day periods as with sst and aod was not valid for the cloud parameters due to the short timescale of cloud development and decay. Even using data combined from both MODIS satellites would exceed this timescale. To compare high aerosol (dirty) air and low aerosol (clean) air clouds, each terra/aqua pass was treated as a synoptic snapshot. Each gridpoint was examined first by aod. Points with $aod > 0.5$ were considered dirty, and points with $aod < 0.2$ were considered clean. Grids were examined pass by pass and day by day for all D-J-F days from Dec. 2002 to Feb. 2007. After separation into clean and dirty categories, the grid points were passed through the cloud mask described above. Those points which were cloudy were grouped into linearly spaced bins by cer or cod value.

The distribution in figure 10 shows that for dirty air, the distribution of cer is much narrower than for clean air. The mode of the distributions are identical, however, the distribution is skewed slightly towards larger radii for the clean air. Figure 11 shows the distribution for cloud optical depth of clean vs. dirty air. Both mode and bulk of the distribution is at higher cod for dirty air than for clean air, suggesting that the second aerosol indirect effect is causing more persistent low clouds where plume aerosols are present.

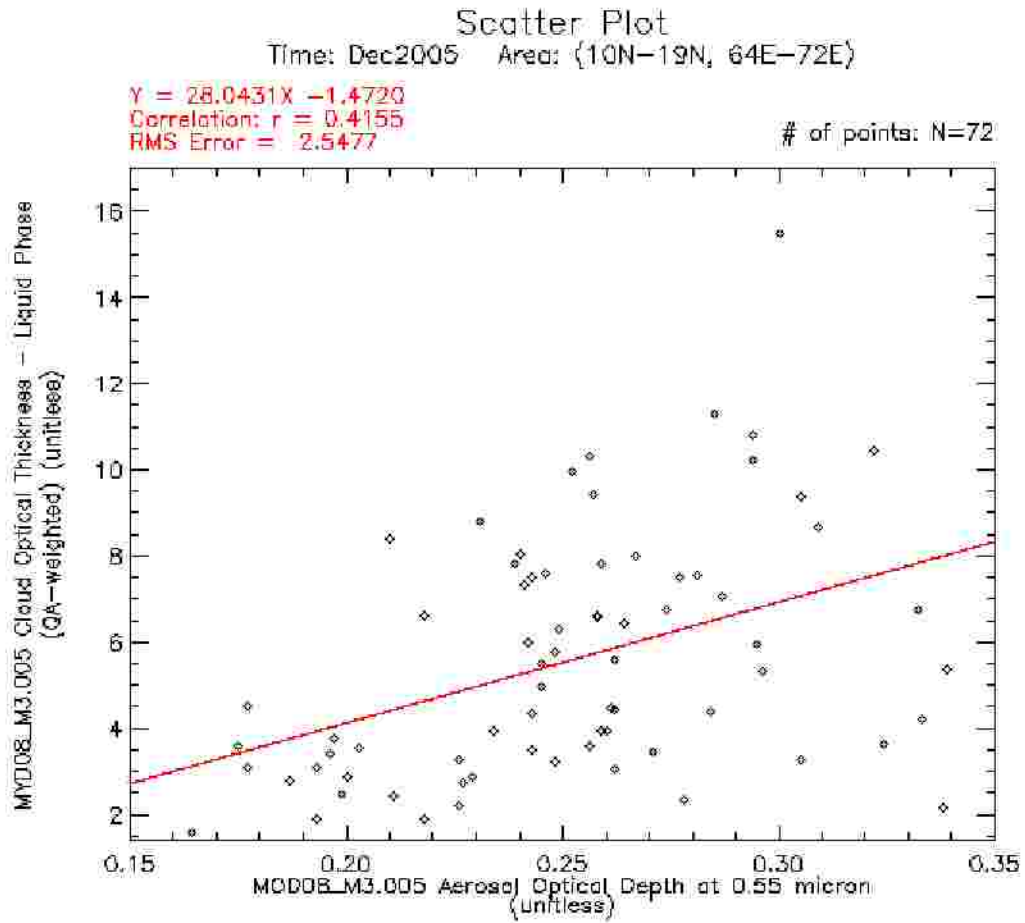
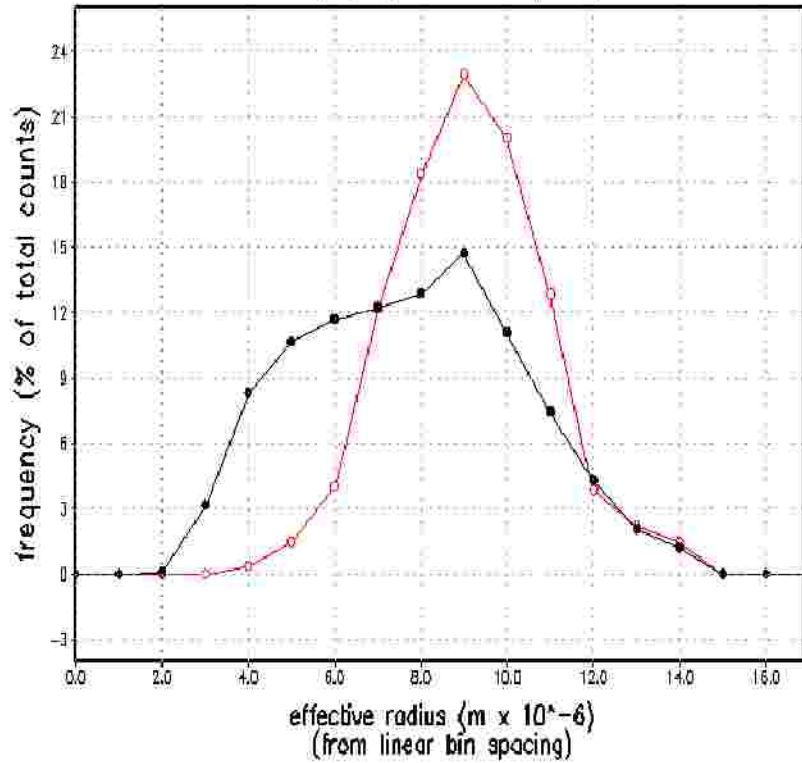


Figure 9: Scatter plot for AOD vs. cloud optical thickness over large area of Arabian sea (10-19 N, 64-72 E) during Dec of 2005 from MODIS. Plot generated by Giovanni. (NASA-GSFC)

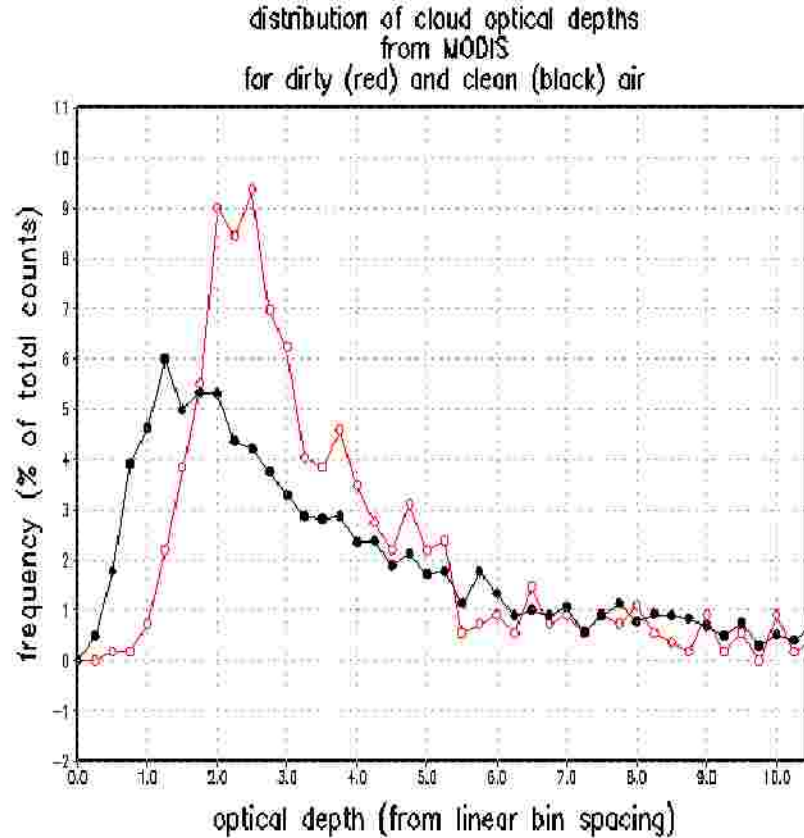
distribution of cloud effective radius
from MODIS
for dirty (red) and clean (black) air



GrADS: COLA/IGES

2007-08-09-13:45

Figure 10: probability distribution of MODIS derived cloud effective radii for dirty air grid points (red) and clean air grid points (black). Taken from 8-18 N, 62-72 E. During D-J-F 2003-2007.



GrADS: COLA/IGES 2007-08-07-14:38
Figure 11: probability distribution of MODIS derived cloud optical depth for dirty air grid points (red) and clean air grid points (black). Taken from 8-18 N, 62-72 E. During D-J-F 2003-2007.

Conclusions:

This study showed that the Bombay Plume is a distinguishable high aerosol concentration feature during the winter monsoon months (defined as D-J-F). The plume originates in West Central India near the cities of Mumbai/Pune. The plume contains a high concentration of very small (diameter <0.5 micron) particles which are likely anthropogenic in origin. During typical D-J-F flow periods, aerosols in the plume are transported over the Arabian Sea, but do not reach a height of more than 3 km.

While the Bombay Plume is over the sea, high aerosol optical depths persist for an average of 5 days. A typical BP is associated with a low level northeasterly jet which stretches nearly across the Arabian Sea. During typical Bombay Plume events, anomaly

sea surface temperatures were observed to lower by more than 0.1 degree Celsius in some areas directly beneath the plume.

While the cloud effective radius was not shown conclusively to increase or decrease in the presence of BP aerosols, it is apparent that a narrower distribution of effective radii is present in areas affected by high aerosol concentration. As the average effective radius over a 1 x 1 degree grid is indicative of the type of cloud present in the grid square, a narrower distribution suggests that there are fewer types of clouds present in that grid square. The distribution of cloud optical depth suggests a shift to more persistent clouds in high aod areas. This is most likely at the expense of deep convective rainy clouds which have shorter lifetimes. More persistent low level clouds over the EAS during winter will have a large impact on the radiation budget in the area. This shift in the radiation budget, combined with sea surface temperature anomalies associated with the Bombay Plume can have a significant impact on regional circulation and rainfall patterns in South Asia.

References:

1. Gradel, T.E. Crutzen, P.J. *Atmospheric Change: an Earth System Perspective*. W. H. Freeman & Co., New York, 1993.
2. Phadnis, Mahesh J., Levy, Hiram II, Moxim, Walter J., On the Evolution of Pollution From South and Southeast Asia During the Winter-Spring Monsoon. *J. Geophys. Res.*, 107, 24, 4790, 2002.
3. J. Lelieveld, P. J. Crutzen, V. Ramanathan, M. O. Andreae, C. A. M. Brenninkmeijer, T. Campos, G. R. Cass, R. R. Dickerson, H. Fischer, J. A. de Gouw, A. Hansel, A. Jefferson, D. Kley, A. T. J. de Laat, S. Lal, M. G. Lawrence, J. M. Lobert, O. L. Mayol-Bracero, A. P. Mitra, T. Novakov, S. J. Oltmans, K. A. Prather, T. Reiner, H. Rodhe, H. A. Scheeren, D. Sikka, J. Williams. "The Indian Ocean Experiment: Widespread Air Pollution from South and Southeast Asia." *Science*. Vol. 291. no. 5506, pp. 1031 – 1036, 2001.
4. Lobert, Jurgen M. Harris, Joyce M. "Trace gases and air mass origin at Kaashidhoo, Indian Ocean." *J. Geophys. Res.*, 107 No. D19, 8013, 2002.
5. Maccherone, Brandon. "About MODIS." NASA-GSFC.
<http://modis.gsfc.nasa.gov/about/>.
6. Hubanks, Paul. "Introduction to MODIS Atmosphere Level-2 Aerosol Products" NASA-GSFC. 6 June 2007.
http://modis-atmos.gsfc.nasa.gov/MOD04_L2/index.html.
7. Hubanks, Paul. "Introduction to MODIS Atmosphere Level-2 Cloud Products" NASA-GSFC. 6 June 2007
http://modis-atmos.gsfc.nasa.gov/MOD06_L2/index.html.
8. Lorentz, Katherine. "A-Train Constellation." NASA-GSFC. 14 June 2007.
<http://www-calipso.larc.nasa.gov/about/atrain.php>.
9. Adler, Robert. "NASA Facts: TRMM Instruments, TRMM Microwave Imager." NASA-GSFC. 21 nov 2006. http://trmm.gsfc.nasa.gov/overview_dir/tmi.html.
10. Krishnamurti, T.N., B. jha, P. J. Rasch, and V. Ramanathan. "A High Resolution Global Reanalysis highlighting the winter monsoon, Part I, Reanalysis Fields." *Meteorol. Atmos. Phys.*, 64, 123-150, 1997.
11. V. Ramanathan, M. V. Ramana. "Persistent, Widespread, and Strongly Absorbing Haze Over the Himaylayan Foothills and the Indo-Gangetic Plains." *Pure Appl. Geophys.* 162, 1609-1626, 2005.

12. K. M. Lau, M. K. Kim, K. M. Kim. "Asian Summer Monsoon Anomalies Induced by Aerosol Direct Forcing: the Role of the Tibetan Plateau." *Climate Dynamics*. 10.1007/s00382-006-0114-z, 2006.
13. Lau, K.-M., and K.-M. Kim. "How nature foiled the 2006 hurricane forecasts," *Eos Trans. AGU*, 88, No. 9. 2007.
14. Takemura, Toshihiko. Kaufman, Yoram. Remer, Lorraine A. Nakajima, Teruyuki. "Two Competing Pathways of Aerosol Effects on Cloud and Precipitation Formation." *J. Geophys. Res.* 34 doi: 10.1029/2006GL028349, 2007.
15. Kaufman, Y. J. Koren, I. Remer, L. Rosenfeld, D. Rudich, Y. "The Effect of Smoke, Dust, and Pollution Aerosol on Shallow Cloud Development over the Atlantic Ocean." *PNAS*, vol.102, no. 32 11207-11212. 2005.
16. Platnick, Steven. King, Michael D. Ackerman, Steven A. Menzel, W. Paul. Baum, Bryan A. Riedi, Jerome C. Frey, Richard A. "The MODIS Cloud Products: Algorithms and Examples From Terra." *IEEE Trans. on Geos. and Remote Sensing*, Vol. 41, No 2, February 2003.